Energy & Environmental Science

RSCPublishing

Environmentally-responsible fabrication of efficient perovskite solar cells from recycled car batteries

Po-Yen Chen,[ab] Jifa Qi,[bc] Matthew T. Klug,[bd] Xiangnan Dang,[bc] Paula T. Hammond[*ab] and Angela M. Belcher[*bce]

Organolead halide perovskite solar cells (PSCs) show great promise as a new large-scale and cost-competitive photovoltaic technology. The power conversion efficiencies have achieved over 15% within 18 months of development, and thus perovskite materials have attracted great attention in photovoltaic research. However, the manufacture of PSCs raises environmental concerns regarding the over-production of raw lead ore, which has harmful health and ecological effects. Herein, we report an environmentally-responsible process to fabricate efficient PSCs by reusing car batteries to simultaneously avoid the disposal of toxic battery materials and provide an alternative, readily-available lead sources for PSCs. Perovskite films, assembled using materials sourced from either recycled battery materials or high-purity commercial reagents, show the same material characterizations (*i.e.*, crystallinity, morphology, optical absorption, and photoluminescence property) and the identical photovoltaic performance (*i.e.*, photovoltaic parameters and resistances of electron recombination), indicating the practical feasibility of recycling car batteries for lead-based PSCs.

Introduction

Organolead halide perovskite materials have recently attracted significant attention as an efficient light harvester and electron transporter for solid-state solar cells.[1,2] Having achieved power conversion efficiencies (PCEs) over 15% with relatively simple and inexpensive fabrication methods, perovskite solar cells (PSCs) show great promise as a new large-scale and cost-competitive photovoltaic technology.[3-7] However, there are health and environmental concerns regarding the current procedures used to mine and refine the lead necessary for synthesizing the organolead halide perovskite materials. The extraction from the raw lead ore, galena, requires high-temperature process over 1400 °C and generates greenhouse gases and dangerous fumes as byproducts.[8] It is challenging to fully enclose the lead vapor/dust escaped from processing facilities, and the toxic materials pose significant hazards to the environment and human health.[9-12] Therefore, alternative lead sources that are abundant, inexpensive, and allow safer extraction and processing procedures are imperative for future manufacture of lead-based PSCs in an environmentally-responsible fashion.

An alternative, readily-available lead source for synthesizing lead halide perovskite materials is the common lead-acid battery, the most widely-used automotive battery.[13,14] The spent materials from lead-acid battery electrodes are currently harvested and reprocessed by manufacturers to produce over half of the new car batteries. On the other hand, rapid development of next-generation energy-storage technology has enabled lithium-based batteries, such as lithium-sulfur and lithium-air devices with higher energy densities, longer lifespans, lighter specific weights, and improved safety compared to the traditional lead-acid design.[15-17] As a result, when the next generation technologies inevitably replace the lead-acid batteries in automobiles, the lead recycling process will be disrupted. The environmentally-hazardous materials from over 250 million retired lead-acid batteries (estimated on the number of registered passenger vehicles in the United States alone)[18] will need to be disposed or repurposed in an environmentally-responsible manner. The benefits of reprocessing these materials to manufacture PSCs are two-folds: the disposal of a large quantity of lead-acid batteries can be managed in an inexpensive way, which provides readily-available lead sources and facilitates the synthesis of perovskite materials for renewable energy production.

Herein, we demonstrate the environmentally-responsible synthetic pathways to reuse car batteries for the fabrication of efficient PSCs. The anodes and cathodes of car batteries are both reused to synthesize lead iodide perovskite materials. In contrast to the traditional lead extraction process, the production of lead components from car batteries involves neither the high-temperature pyrometallurgical process nor the emission of lead vapor/dusts and greenhouse gases to the environment. The lead iodide perovskite films synthesized from car batteries and high-purity reagent demonstrate the same material characterizations (*i.e.*, crystallinity, morphology, optical absorption, and photoluminescence property). The photovoltaic performance of the PSCs fabricated from either

material sources are the same, indicating that device quality is not contingent on the source if proper processing procedures are followed. In addition, the resulting PSCs are measured by electrochemical impedance spectroscopy (EIS), and the similarity between the resistances of electron recombination indicates that the electron-transport properties of the lead iodide perovskite from two different sources are identical. Moreover, an economic analysis shows that the lead from one car battery will enable the fabrication of ~709.0 m^2 perovskite-based solar panels, which can support the electricity usage of ~30.2 US residential units in Las Vegas, Nevada (average daily electricity consumption for an United States residential unit is 29.1 kWh day^{-1}).[19-21] With this technique, the time required to find a lead replacement for PSCs can be further elongated.

Experimental

Materials synthesis. Lead, lead dioxide (PbO$_2$), lead iodide (PbI$_2$), potassium iodide (KI), 2-propanol (IPA), nitric acid (HNO$_3$), acetic acid, N,N-dimethylformamide (DMF), hydrochloric acid (HCl), hydroiodic acid (HI), methylamine (CH$_3$NH$_2$), zinc powder, and titanium isopropoxide (TTIP), titanium tetrachloride (TiCl$_4$) were purchased from Sigma-Aldrich. Lead oxide (PbO) was purchased from Alfa-Aesar. Fluorine-dope tin oxide (FTO) glass (TEC 15, thickness = 2.2 mm) was purchased from Pilkington. 2,2',7,7'-Tetrakis(N,N-p-dimethoxyphenylamino)-9,9'-spirobifluorene (Spiro-MeOTAD) was purchased from SunaTech Incorporation (China). Gold target was purchased from R. D. Mathis Company. All reagents were used as received and without further purification. All water was deionized (18.2 M□, mill-Q pore). CH$_3$NH$_3$I was synthesized according to a reported procedure[3]. HI solution (30 mL, 57 wt.% in water) and CH$_3$NH$_2$ solution (27.8 mL 40 wt.% in methanol) were mixed and stirred in the ice bath for 2 hours. CH$_3$NH$_3$I was then crystallized by removing the solvent in an evaporator, washing three times in diethyl ether for 30 minutes, and filtering the precipitate. The material, in the form of white crystals, was then dried in vacuum at 60 °C for 24 hours. It was then kept in a dark, dry environment until further use.

Harvesting material from the anodes and cathodes of car battery. The recycling process of anodes and cathodes of car battery was conducted by automobile maintenance station (Hung-Fu Incorporation, Taiwan). Car battery (Yuasa Batteries, standard type, 12-V) was disconnected from a Japanese automobile (Nissan Cefiro). The acid electrolyte was poured out and carefully collected, and the electrodes as well as the inner wall of car battery were rinsed several times by clean water. CAUTIONS: the electrolyte contains concentrated sulfuric acid (~4.2 M), and gloves, safety glasses, and lab coat are highly required during this process. The as-obtained car battery was dried in the ambient condition for 3 days. The dry car battery was disassembled from the top lid and then sawed from the sides to extract the electrode panels. After disassembling, the lead-derived materials (*i.e.*, lead and PbO$_2$) were scratched off from the current collectors separately, and washed with dilute HCl (0.1 M) and clean water sequentially. The collected materials were ground into powders for further synthesis.

Synthesizing PbI$_2$ from the collected materials of car battery. The lead-related materials from anodes (lead) and cathodes (PbO$_2$) were conducted in different synthetic pathways to generate PbI$_2$ in high yields. PbO$_2$ powder was first roasted at 600 °C for 5 hours to decompose it into PbO, and the color of the powder was changed from dark-brown to yellow.

After roasting, the PbO powder was easily dissolved in dilute acetic acid (1.9 M) to release lead(II) ion (Pb^{2+}) in the solution. Pb powder from anodes was reduced into dilute HNO$_3$ (0.8 M) and Pb^{2+} was released completely into the solution (CAUTIONS: this reaction generated reddish and toxic nitrogen dioxide gas and must be conducted in the fume hood). After Pb^{2+} was present in the solutions, the solutions are mixed with KI solution. The yellow precipitate of PbI$_2$ was collected, further washed by cold water and dried in a vacuum chamber overnight. The as-synthesized PbI$_2$ was further ground into fine powder for further synthesis.

Synthesizing lead iodide perovskite materials. PbI$_2$ was dissolved in DMF at a concentration of 462 mg mL^{-1} (~1 M) under stirring at 80 °C. The solution was kept at 80 °C during the whole procedure. The FTO substrates were then infiltrated with PbI$_2$ by spin-coating the solution at 6500 r.p.m. for 60 seconds and dried at 80 °C for 1 hour. After cooling to room temperature, the films were dipped in a solution of CH$_3$NH$_3$I in IPA (10 mg mL^{-1}) for 1 minute, rinsed with IPA and dried at 90 °C for 30 minutes. The optical absorption spectroscopy measurements were performed using a Beckman Coulter DU800 UV-Vis spectrophotometer. Surface morphology of the perovskite nanocrystals were investigated using a scanning electron microscope (SEM, Helios Nanolab 600 Dual Beam Focused Ion Beam System) operating at 10.0 kV for medium and high resolution imaging. Powder X-ray diffraction (XRD) patterns were collected (PANanalytical Multipurpose Diffractometer, Cu Kα radiation operated at 40 kV and 40 mA) using a step size of 0.02° with 6.0° per minute scan speeds under the following settings: 2° of anti-scatter slit, 6 mm of irradiated length of automatic mode and 0.04 rad of soller slit. Steady-state PL spectra were measured at room temperature on a HORIBA Jobin-Yvon Nanolog spectrometer equipped with a 450 W xenon arc lamp, single-grating excitation and double-grating emission monochromators (spectral resolution 1 nm) and a Hamamatsu R928 photomultiplier tube. Time-resolved photoluminescence (PL) measurements were performed using a time-correlated single-photon-counting option on the Nanolog (HORIBA Jobin-Yvon, FluoroHub). 610 nm light pulse from a laser NanoLED (the half-width at half-maximum (HWHM) is 1.39 ns, average power 2.4 pJ pulse^{-1}) was used to as excitation source. The emission photons dispersed by a double-grating emission monochromator was collected with a Hamamatsu R928 single-photon-counting detector. Time-resolved PL data was analyzed with software DAS6 (HORIBA Jobin-Yvon).

Device fabrication. The FTO-coated glass substrates were patterned by photolithography and etched by zinc powder and HCl (2.0 M) for 5 minutes. The patterned substrates were rinsed with dilute hydrofluoric acid (5.0 wt.%) and cleaned by ultrasonication in an aqueous soap solution, milli-Q water, acetone, and IPA sequentially. The clean substrates were subjected to an O$_3$/ultraviolet treatment for 30 minutes. To make a dense titanium dioxide (TiO$_2$) blocking layer, the FTO glasses were coated with 0.15 M TTIP in ethanol solution by the spin-coating method at 3000 r.p.m. which were heated at 500 °C for 30 minutes. After the deposition, the substrates were treated in a 0.04 M aqueous solution of TiCl$_4$ for 30 minutes at 80 °C, rinsed with milli-Q water and dried at 500 °C for 30 minutes. The TiO$_2$ paste with 20-nm-sized particles was synthesized according to a reported procedure.[22] The 500-nm-thick TiO$_2$ films are fabricated by spin-coating the paste at 2500 r.p.m. for 60 seconds. After drying at 100 °C, the TiO$_2$ films were gradually heated to 500 °C for 30 minutes and cooled to room temperature. Lead iodide perovskite nanocrystals (*i.e.*,

$CH_3NH_3PbI_3$) was deposited on the TiO_2 films according to the procedure above. The hole-transporting material was then deposited by spin-coating at 4000 r.p.m. for 30 seconds. The spin-coating solution was prepared by dissolving 72.3 mg spiro-MeOTAD, 28.8 μL 4-tert-butylpyridine, 17.5 μL of a stock solution of 520 mg mL^{-1} lithium bis(trifluoromethylsulphonyl) imide in acetonitrile in 1 mL chlorobenzene. Finally, 80 nm of gold was thermally evaporated on top of the device.

Characterization of perovskite solar cells (PSCs). Photovoltaic measurements were performed using an AM 1.5 solar simulator (Photo Emission Tech.). The power of the simulated light was calibrated to 100 mW cm^{-2} by using a reference silicon photodiode with a power meter (1835-C, Newport) and a reference silicon solar cell to reduce the mismatch between the simulated light and AM 1.5. J-V curves were obtained by applying an external bias to the cell and measuring the generated photocurrent with a Keithley model 2400 digital source meter. The voltage step and delay time of photocurrent were 10 mV and 40 ms, respectively. Electrochemical impedance spectroscopy (EIS) of PSCs was measured using a Solartron 1260 frequency response analyzer. The photoanode was connected to the working electrode. The platinum electrode was connected to the auxiliary electrode and reference electrodes. The impedance measurements were carried out at forward bias in dark conditions. The spectra were measured at various forward bias voltages in the frequency range ~0.1 Hz to ~1 MHz with oscillation potential amplitudes of 10 mV at room temperature. The applied forward bias voltage was changed by 50 mV steps from 1000 mV to 0 mV. The obtained impedance spectra were fit to the reported model with Z-view software (v3.2b, Scribner Associates).[23-25]

Results and discussion

Fig. 1 provides a flowchart that compares two processes to synthesize perovskite materials. The conventional process begins with freshly mined galena whereas our process begins with spent car batteries. The traditional extraction of lead from galena involves two high-temperature processes: (1) a pre-roasting oxidation step (>1400 $^{\circ}$C) to turn galena into lead oxides (PbO_x) and (2) a pyrometallurgical process (>1200 $^{\circ}$C) to reduce PbO_x to lead.[26] Both procedures require high-energy input and generate carbon dioxide (CO_2) as an undesired byproduct. Furthermore, lead vapor and dust can escape with the exhaust into the atmosphere, which can then accumulate in the surroundings and endanger human and ecological health.[23,24] In contrast to the complicated, energy-intensive, and potentially hazardous pathways starting from galena, the production from car batteries is more straightforward and with minimal emission of harmful byproducts. The synthesis occurs at a lower temperature (~600 $^{\circ}$C) and does not release any CO_2. By reusing spent lead-based materials from car batteries, emerging PSC manufacturers could source raw materials from existing waste rather than mining and processing new ore with the aforementioned traditional methods.

Fig. 2 and Movie S1 show the detailed synthesis of lead iodide perovskite materials from a spent lead-acid car battery. The process includes three steps: (1) harvesting material from the anodes and cathodes of car battery, (2) synthesizing PbI_2 from the collected materials, and (3) depositing lead iodide perovskite nanocrystals. First, a used 12-V lead-acid battery is disconnected from an automobile. After disconnection, the acid electrolyte (containing concentrated sulfuric acid) is diluted

with water and then poured out. The electrodes are further rinsed with water several times and air-dried for two days. The dry car battery is then disassembled with jigsaw from the top casing to avoid damaging the electrodes. After removal of the casing, the electrode panels become accessible. The disassembly process is conducted by a professional technician, and the toxic waste materials are properly collected and disposed. The disassembled lead-acid battery includes 36 anodes (lead) and 36 cathodes (PbO_2), with the dimension of each electrode around 15 cm × 15 cm × 0.25 cm. The lead-derived materials on the current collectors are scraped off and rinsed with dilute HCl. The collected materials are then ground into fine powders for further processing. As shown in Fig. S1a,b, the as-obtained lead and PbO_2 powders produce identical XRD patterns to the high-purity chemicals of Sigma-Aldrich (#391352, >99.95%) and Alfa Aesar (#12483, >97.0%).

To synthesize PbI_2 with high yields, the as-obtained lead and PbO_2 powders are treated with different synthetic pathways. Because of the low reactivity of PbO_2 in HNO_3, the generation of Pb^{2+} is inefficient and the yield is lower than 5% (equation 1).

$$2PbO_2(s) + 4HNO_3(aq.) \rightarrow 2Pb(NO_3)_2(aq.) + 2H_2O(l) + O_2(g) \tag{1}$$
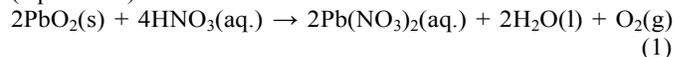
As a result, PbO_2 requires a composite treatment: first, the powder is sintered at 600 $^{\circ}$C for 5 hours in air to decompose PbO_2 into PbO (equation 2).

$$PbO_2(s) \rightarrow PbO(s) + 1/2\ O_2(g) \tag{2}$$

The complete transformation is confirmed visually by the color change from dark red to yellow, and quantitatively by matching the XRD pattern of the as-obtain PbO (Fig. S1c) to that of the high-purity PbO of Sigma-Aldrich (#15338, >99.0%). The as-synthesized PbO powder is highly soluble in dilute acetic acid (1.9 M), and Pb^{2+} is generated efficiently in the solution. Lead powder from anodes is reduced by dilute HNO_3 (0.8 M) and the yield of Pb^{2+} is close to 100% (equation 3).

$$Pb(s) + 4HNO_3(aq.) \rightarrow Pb(NO_3)_2(aq.) + 2H_2O(l) + 2NO_2(g) \tag{3}$$
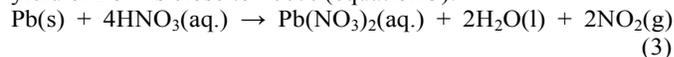
After both electrodes are transformed into Pb^{2+} completely, the solutions are both mixed with the potassium iodide (KI) solution. Pb^{2+} reacts with I^- and yields insoluble yellow PbI_2 products immediately. After washing with cold water, the as-obtained PbI_2 is collected and dried in a vacuum oven overnight. The resulting PbI_2 from car batteries are characterized by XRD analysis, and the XRD pattern are identical to that of the high-purity PbI_2 (Sigma-Aldrich, #211168, >99%) (Fig. S1d).

After PbI_2 is synthesized, lead iodide perovskite nanocrystals are synthesized by the reported sequential deposition process.[3] PbI_2 is introduced into the TiO_2 nanoparticle-based films by spin-coating a solution of PbI_2 in DMF at 80 $^{\circ}$C. The PbI_2/TiO_2 composite films are dipped into a solution of CH_3NH_3I in IPA, and the films change color immediately from yellow to dark brown, indicating the formation of lead iodide perovskite (*i.e.*, $CH_3NH_3PbI_3$). XRD pattern of the perovskite nanocrystals from car batteries exhibits the same crystallinity to the one from high-purity PbI_2 of Sigma-Aldrich (Fig. 3a).

The study of photophysical properties enables the characterization of organometallic lead halide perovskite and the understanding of the charge photogeneration and recombination mechanisms.[27] To evaluate the light-harvesting capability between the lead halide perovskite materials synthesized from car batteries and commercial PbI_2, the optical absorbance and the photoluminescence (PL) response of the

fabricated thin films are characterized. The thin films synthesized from both sources are prepared under the same parameters as the fabricated devices (*e.g.*, the concentration of PbI_2 and methylamine iodide solutions, the spin-coating speed/time, and the drying temperature/time). As a result, the thickness of the PbI_2- and perovskite-coated thin films for the optical and PL measurements is almost the same as the thickness in the fabricated devices.

The absorption spectra of PbI_2- and perovskite-coated TiO_2 films (from car batteries and high-purity PbI_2) are plotted in Fig. 3b. The absorption of both PbI_2-coated TiO_2 films is under 450 nm, and the resulting perovskite-coated TiO_2 films show an increased absorbance and a broad absorption spectra ranging from below 400 nm to 850 nm. The PL spectra of lead iodide perovskite nanocrystals deposited on mesoporous alumina oxide (Al_2O_3) thin films from both sources exhibit a strong single emission band (Fig. 3b). The spectral features of the samples from both sources are the same: the spectral peak position is both at 747 ± 2 nm (1.66 eV), and the half-width at half-maximum (HWHM) is both 130 ± 3 meV. Also, the integrated intensities are same for both preparations. The strong emission is attributed to the radiative recombinations of photogenerated carriers localized in organolead iodide perovskite nanocrystals.[27] Furthermore, the dynamics of PL of both organolead iodide perovskite nanocrystals is investigated by monitoring the PL decay at 747 nm (shown in Fig. S2). All samples exhibit a single exponential relaxation process with the same lifetime of 1.00 ± 0.09 ns.

The identical absorption and PL spectral properties demonstrate that materials sourced from batteries and high-purity reagents display the same optical transitions from ground states to excited states, and vice versa. The similarity indicates that both batches of nanocrystals display the same chemical structure and the identical light-absorption capability. The crystallized morphologies of both perovskite nanocrystals are visualized by scanning electron microscopy (SEM), and the images are shown in Fig. 3c,d. In Fig. 3c,d, the morphologies synthesized from both sources are similar with the crystal size from 20 nm to 400 nm, and the film coverage, as analyzed by image processing (*ImageJ*), is approximately 100%.

After the PSCs are assembled, the photovoltaic performance of the PSCs fabricated from car batteries and high-purity PbI_2 are both tested under AM 1.5G illumination conditions (100 mW cm^{-2}). To compare the photovoltaic performance between the PSCs fabricated from car batteries and high-purity PbI_2, a histogram of the PCE from batches of ~32 PSCs is shown in Fig. 4a. Histogram plots of solar cell performance parameters, including open-circuit voltage (V_{OC}), short-circuit current (J_{SC}), and fill factor (FF), are also shown in Fig. S3. In addition, Fig. 4b presents the average PCE and the highest PCE from batches of PSCs. The current density-voltage (J-V) curves of the most efficient PSC are plotted in Fig. 4c, and the related photovoltaic parameters are listed in Table 1. From these photovoltaic measurements, it is clearly demonstrated that the PSCs fabricated from either of the two sources show similar photovoltaic performance, indicating car batteries can serve as an alternative lead sources for the environmentally-responsible fabrication of lead-based PSCs.

Furthermore, the two kinds of PSCs are characterized by EIS. Nyquist plots of solid-state PSCs fabricated from car batteries and high-purity PbI_2 at 550 mV and 800 mV are both shown in Fig. S4. Nyquist plots at 800 mV (Fig. S4b,c) and 550 mV (Fig. S4e,f) are both enlarged to observe the detailed features in intermediate and high frequency region. At high frequency (Fig. S4c,f), the gold/hole-transporting material interface is similar to the interface between the liquid electrolyte and the counter electrode in dye-sensitized solar cells (DSCs).[28] The resistance at this interface remains almost the same over the whole applied voltage range, and the resistance slightly reduce at higher applied voltage, which is often observed in the literature.[23] Moreover, at intermediate frequency (Fig. S4b,e), the straight characteristics of transmission line, which is normally observed in the nanostructured photoanodes, are seen. The transmission lines merge into the semicircles representing the recombination resistance at lower frequency. After PSCs from either of the two sources are characterized by EIS, the spectra are analyzed by following the reported model.[23-25,29] The recombination resistances of the devices fabricated from car batteries and high-purity PbI_2 are shown in Fig. 4d. The similarity of the resistances of electron recombination in Fig. 4d indicates that the electron-transport properties of the lead iodide perovskite synthesized from the two different sources are identical. From these photovoltaic measurements, it is clearly demonstrated that car batteries can serve as an alternative lead sources for the environmentally-responsible fabrication of lead-based PSCs. More details regarding fitting the EIS data are provided in Experimental section and Supporting Information.

Finally, to highlight the feasibility of producing perovskite materials using this environmentally-responsible approach, a simple economic analysis is performed. The average weight of a lead-acid battery is around 18.1 kg, and the lead-related materials are responsible for about 60% of the weight (~10.9 kg), while the other 40 wt.% is comprised of the liquid electrolyte, outer casing, separators, and current collectors[13,14]. It is assumed that the weight of the anodes and cathodes are the same (5.4 kg). Based on the experiments performed, the yields from lead and PbO_2 electrodes to PbI_2 are 95.6% and 97.8%, respectively, which is expected to produce 21.5 kg of PbI_2. By considering the structure of PSCs (~500 nm-thick PbI_2 coating) and the material loss during the spin-coating process (~89.6%), 21.5 kg of PbI_2 enables the fabrication of ~709.0 m^2 PSCs.

Since the solar illumination varies in different locations, multiple locations (*e.g.*, Cambridge, MA, US; Las Vegas, NV, US; London, UK) are chosen and analyzed. If the PCE achieves ~15% (close to the reported PCEs of PSCs in the literature),[3,4] the resulting perovskite solar panels can generate ~398.8 kWh day^{-1} based on the annual average illumination in MIT, Cambridge, Massachusetts (~3.75 kWh m^{-2} day^{-1}).[19] The generated energy meets the electricity usage for ~13.7 US residential units (average daily electricity consumption for an United States residential unit is 29.1 kWh day^{-1}).[20,21] In the other words, ~51.7 m^2 perovskite solar panels are required to be installed to provide sufficient electricity for the daily usage of a single US residential unit in Cambridge.[20,30,31] If the perovskite solar panels are installed in Las Vegas, Nevada (the annual average illumination is ~8.25 kWh m^{-2} day^{-1}),[19] ~30.2 US residential units can be powered, and ~23.5 m^2 solar panels are required for each household in this region. In addition, the same-sized perovskite solar panels installed in London (the annual average illumination is ~3.11 kWh m^{-2} day^{-1}),[32] ~26.1 UK residential units can be powered (average daily electricity consumption for an United States residential unit is ~12.7 kWh day^{-1}),[33] and ~27.2 m^2 solar panels are required for each household in this region.

Moreover, using the United State as an example, to power the whole United States (3.9×10^{12} kWh $year^{-1}$),[34] about 12.2 million recycled car batteries, which is ~12% of the spent

American vehicle and industrial batteries in 2007,[35] are required to fabricate 8634 km^2-sized perovskite solar panels installed in Nevada, which is only ~3% of its total area. With great focus on improving the performance of PSCs in academia and installing the recycled system for PbI_2 solution during spin-coating in industry, these numbers can be further calibrated and improved. With the assumption of a 25-year lifetime for the PSCs, the lead resourced from recycled car batteries in the whole US industry for the PSCs could power the US over 200 years. In addition, we are pursuing the recycling and reusing the lead component within the used perovskite solar panels. With these approaches, the time required to find a lead replacement for high-efficiency PSCs can be further elongated.

Conclusions

We have demonstrated an environmentally-responsible synthetic pathway to reuse car batteries for the fabrication of efficient PSCs. Both the anodes and cathodes of car batteries serve as material sources for the synthesis of lead iodide perovskite materials. In contrast to the traditional lead extraction process, our synthesis pathway from recycled battery material occurs at a lower temperature (600 $^\circ$C) and does not include the hazardous emission of lead vapor/dust and CO_2 to the environment. The lead iodide perovskite materials synthesized from car batteries and high-purity reagents demonstrate identical material characterizations. The photovoltaic performance of the PSCs synthesized by each route is the same, which demonstrates that device quality does not suffer from the materials sourced from spent car batteries. Also, EIS measurements reveal that each device type displays the same resistances of electron recombination, indicating that the electron-transport properties of the lead iodide perovskite are identical. Finally, a simple economic analysis reveals that a single lead-acid car battery can supply enough lead material for the fabrication of ~709 m^2 PSCs, which can provide enough electricity to power ~30.2 US residential units in Las Vegas, Nevada. With these techniques, the time required to find a lead replacement for PSCs can be further elongated. The environmentally-responsible fabrication is expected to be broadly applicable not only to the PSC technology but also other applications (including but not limited to lead sulfide (PbS) quantum-dot solar cells, lead zirconate titanate (PZT) piezoelectric devices), and the recycling strategy will have important industrial implications in the future.

Notes and references
[a] Department of Chemical Engineering, Massachusetts Institute of Technology, Cambridge, MA 02139 (USA)
[b] The David H. Koch Institute for Integrative Cancer Research, Massachusetts Institute of Technology, Cambridge, MA 02139 (USA)
[c] Department of Materials Science and Engineering, Massachusetts Institute of Technology, Cambridge, MA 02139 (USA)
[d] Department of Mechanical Engineering, Massachusetts Institute of Technology, Cambridge, MA 02139 (USA)
[e] Department of Biological Engineering, Massachusetts Institute of Technology, Cambridge, MA 02139 (USA)
[*] Address correspondence to hammond@mit.edu and belcher@mit.edu.

1. G. Xing, N. Mathews, S. Sun, S. S. Lim, Y. M. Lam, M. Grätzel, S. Mhaisalkar and T. C. Sum, *Science*, 2013, **342**, 344.
2. S. D. Stranks, G. E. Eperon, G. Grancini, C. Menelaou, M. J. P. Alcocer, T. Leijtens, L. M. Herz, A. Petrozza and H. J. Snaith, *Science*, 2013, **342**, 341.
3. J. Burschka, N. Pellet, S.-J. Moon, R. Humphry-Baker, P. Gao, M. K. Nazeeruddin and M. Grätzel, *Nature*, 2013, **499**, 316.
4. M. Liu, M. B. Johnston and H. J. Snaith, *Nature*, 2013, **501**, 395.
5. H. S. Kim, C. R. Lee, J. H. Im, K. B. Lee, T. Moehl, A. Marchioro, S. J. Moon, R. Humphry-Baker, J. H. Yum, J. E. Moser, M. M. Grätzel and N. G. Park, *Sci. Rep.*, 2012, **2**, 591.
6. M. M. Lee, J. Teuscher, T. Miyasaka, T. N. Murakami and H. J. Snaith, *Science*, 2012, **338**, 643.
7. R. F. Service, *Science News*, 2014.
8. C. A. Sutherland, E. F. Milner, R. C. Kerby, H. Teindl, A. Melin and H. M. Bolt, in *Ullmann's Encyclopedia of Industrial Chemistry*, Wiley, 2000.
9. B. P. Lanphear, T. D. Matte, J. Rogers, R. P. Clickner, B. Dietz, R. L. Bornschein, P. Succop, K. R. Mahaffey, S. Dixon, W. Galke, M. Rabinowitz, M. Farfel, C. Rohde, J. Schwartz, P. Ashley and D. E. Jacobs, *Environ. Res.*, 1998, **79**, 51.
10. H. W. Mielke and P. L. Reagan, *Environ. Health Perspect.*, 1998, **106**, 217.
11. K. Koller, T. Brown, A. Spurgeon and L. Levy, *Environ. Health Perspect.*, 2004, **112**, 987.
12. S. Tong, Y. E. Schirnding and T. Prapamontol, *Bull. World Health Organ.*, 2000, **78**, 1068.
13. D. A. J. Rand, J. Garche, P. T. Moseley and C. D. Parker, *Valve-Regulated Lead-Acid Batteries.*, Elsevier, Amsterdam, 2004.
14. D. Pavlov, *Lead-Acid Batteries: Science and Technology*, Elsevier, Amsterdam, 2011.
15. M. Armand and J. M. Tarascon, *Nature*, 2008, **451**, 652.
16. P. G. Bruce, S. A. Freunberger, L. J. Hardwick and J.-M. Tarascon, *Nat. Mater.*, 2012, **11**, 19.
17. V. Etacheri, R. Marom, R. Elazari, G. Salitra and D. Aurbach, *Energy Environ. Sci.*, 2011, **4**, 3243.
18. *Number of U.S. aircraft, vehicles, vessels, and other conveyances*, U.S. Department of Transportation, 2011.
19. *PV Solar Radiation (10 km) - Static Map*, NREL.
20. *Electric sales, revenue, and average price*, U.S. Department of Transportation, 2011.
21. *Average monthly residential electricity consumption, prices, and bills by state*, U.S. Energy Information Administration 2012.
22. S. Ito, T. N. Murakami, P. Comte, P. Liska, C. Grätzel, M. K. Nazeeruddin and M. Grätzel, *Thin Solid Films*, 2008, **516**, 4613.
23. A. Dualeh, T. Moehl, N. Tétreault, J. Teuscher, P. Gao, M. K. Nazeeruddin and M. Grätzel, *ACS Nano*, 2014, **8**, 362.
24. V. Gonzalez-Pedro, E. J. Juarez-Perez, W.-S. Arsyad, E. M. Barea, F. Fabregat-Santiago, I. Mora-Sero and J. Bisquert, *Nano Lett.*, 2014, **14**, 888.
25. H.-S. Kim, I. Mora-Sero, V. Gonzalez-Pedro, F. Fabregat-Santiago, E. J. Juarez-Perez, N.-G. Park and J. Bisquert, *Nat. Commun.*, 2013, **4**.
26. *Energy and environmental profile of the U.S. mining industry*, U.S. Department of Energy (DOE), 2002.
27. F. Deschler, M. Price, S. Pathak, L. E. Klintberg, D.-D. Jarausch, R. Higler, S. Hüttner, T. Leijtens, S. D. Stranks, H. J. Snaith, M. Atatüre, R. T. Phillips and R. H. Friend, *J. Phys. Chem. Lett.*, 2014, **5**, 1421.
28. J. Bisquert, *J. Phys. Chem. B*, 2001, **106**, 325.
29. F. Fabregat-Santiago, J. Bisquert, L. Cevey, P. Chen, M. Wang, S. M. Zakeeruddin and M. Grätzel, *J. Am. Chem. Soc.*, 2008, **131**, 558.

30. *Electric power annual*, U.S. Energy Information Administration, 2013.

31. *Historical average annual prices by state by type of customer and provider*, U.S. Energy Information Administration, 2012.

32. PVGIS solar map.

33. *Household electricity consumption (kWh/year)*, Would Energy Council, 2010.

34. *International energy statistics, total electricity net consumption (billion kilowatthours)*, U.S. Energy Information Administration, 2010.

35. E. Rosenthal, W. A. Lehren, K. Zabludovsky and D. Agren, in *The New York Times*, 2011.

Energy & Environmental Science Accepted Manuscript
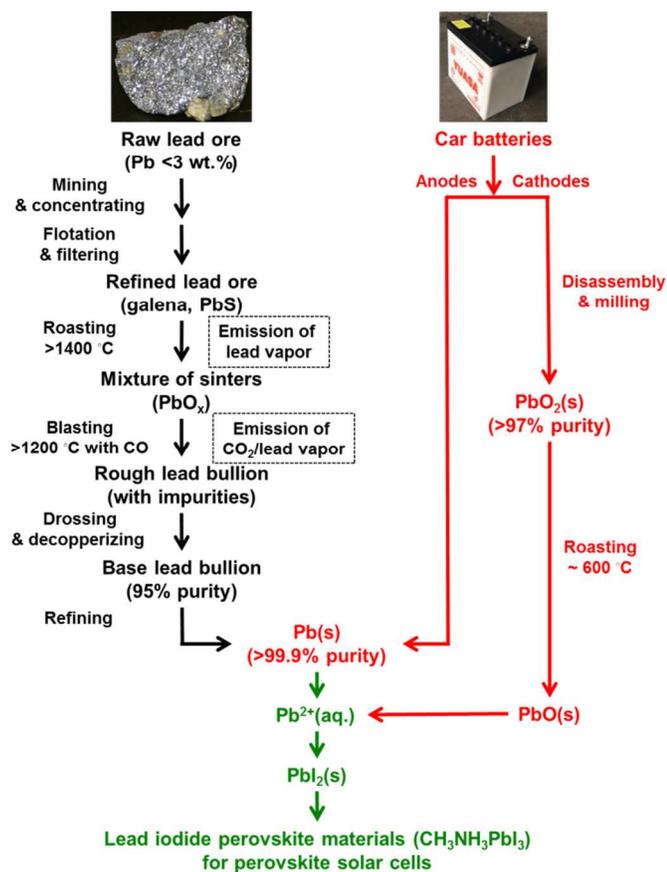
Fig. 1 Schematic illustration of the process to synthesize lead iodide perovskite materials from raw lead ore and from spent car batteries. The black, red, green arrows and texts describe the steps and products in the synthetic processes from raw lead ore to high-purity lead, from car batteries to high-purity lead (or Pb^{2+}), and from high-purity lead to lead iodide perovskite materials, respectively. Compared to the complicated and high-temperature synthetic pathways from raw lead ore, the production of lead iodide perovskite from car batteries is a much more straightforward procedure with minimal emission of harmful byproducts.
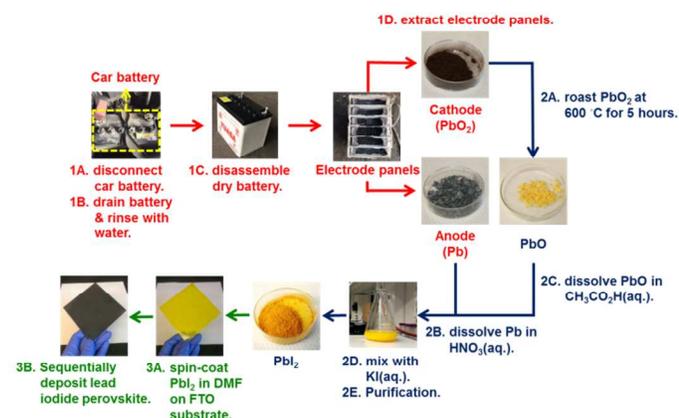
Fig. 2 Synthetic process of lead iodide perovskite materials from a lead-acid car battery. The process includes three steps: (1) harvesting material from the anodes and cathodes of car battery

(red); (2) synthesizing PbI_2 from the collected materials (blue); (3) depositing lead iodide perovskite nanocrystals (green). For the greater details, please refer to Movie S1. The spent car batteries can serve as readily-available alternative lead sources for the environmentally-responsible fabrication of lead-based PSCs.
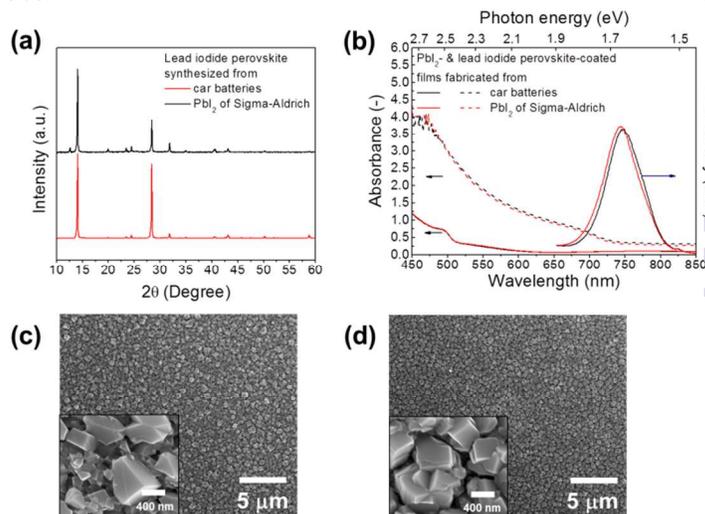
Fig. 3 Materials characterizations. (a) XRD analysis on the lead iodide perovskite nanocrystals fabricated from car batteries and high-purity commercial PbI_2. (b) Optical properties: absorption spectra of the PbI_2-coated (dash lines) and lead iodide perovskite-coated (solid lines) TiO_2 films from car batteries and high-purity commercial product; PL spectra of lead iodide perovskite films (solid lines) coated on mesoporous Al_2O_3 substrates fabricated from car batteries and high-purity commercial PbI_2. SEM images of the lead iodide perovskite nanocrystals synthesized from (c) high-purity commercial PbI_2 and (d) car batteries. The identical XRD pattern, absorption, PL spectral property, and crystallized morphology of both perovskite materials indicate the same chemical structure.
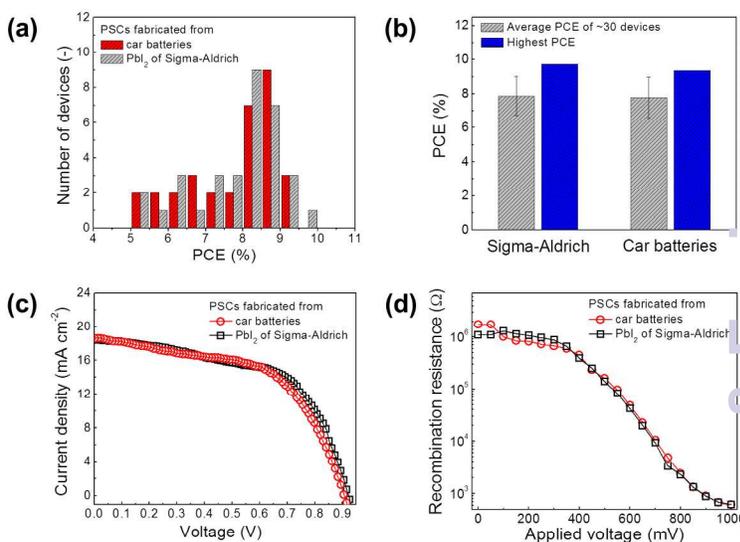
Fig. 4 Device characterizations. (a) the static data of PCE distribution for multiple batches of PSCs (~65 devices in total). Each batch is around 10-12 devices. (b) Average efficiency and their highest performance of ten devices fabricated from car

batteries and high-purity commercial PbI_2. (c) J-V curves of the most efficient devices and the related photovoltaic parameters listed in Table 1. (d) Resistance of electron recombination of the device fabricated from car batteries and high-purity commercial PbI_2. The resistances are determined from impedance measurements conducted in the dark. The photovoltaic performance and the resistances of electron recombination of the PSCs synthesized by each route are the same, which demonstrates that device quality does not suffer from the materials sourced from spent car batteries.

Table 1 Photovoltaic parameters. The related photovoltaic parameters (including PCE, open-circuit voltage (V_{OC}), short-circuit current density (J_{SC}), and fill factor (FF)) in Fig. 4b.

PSC fabricated from	PCE (%)	V_{OC} (mV)	J_{SC} (mA cm^{-2})	FF (%)
PbI_2 (Sigma-Aldrich)	9.73	921	18.42	57.3
Car batteries	9.37	910	18.60	55.4

Table of Content (TOC)
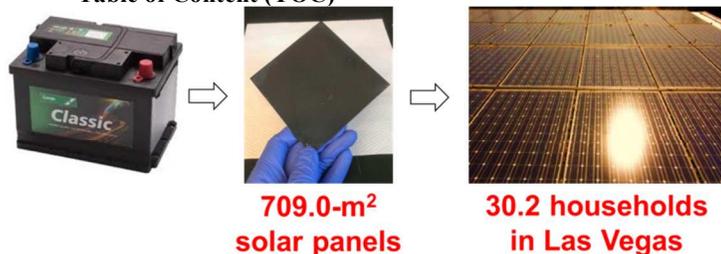
709.0-m² solar panels → 30.2 households in Las Vegas

The report presents a process to fabricate perovskite hybrid solar cells in an environmentally-responsible fashion by recycling lead materials from the spent car batteries.

**709.0-m²
solar panels**

**30.2 households
in Las Vegas**

The report presents a process to fabricate perovskite hybrid solar cells in an environmentally-responsible fashion by recycling lead materials from the spent car batteries.